Molecular Crystals and Liquid Crystals
Publication details, including instructions for authors and subscription information:
http://www.tandfonline.com/loi/gmcl16

Determination of the Surface Tilt Angle by Attenuated Total Reflection

G. J. Sprokel [a] , R. Santo [a] & J. D. Swalen [a]
[a] IBM Research Laboratory, San Jose, California, 95193, U.S.A.
Version of record first published: 14 Oct 2011.

Mol. Cryst. Liq. Cryst., 1981, Vol. 68, pp. 29–38
0026-8941/81/6801-0029 $06.50/0

Printed in the United States of America

Determination of the Surface Tilt Angle by Attenuated Total Reflection†

G. J. SPROKEL, R. SANTO and J. D. SWALEN
IBM Research Laboratory, San Jose, California 95193, U.S.A.

(*Received May 1, 1980*)

Thin SiO_2 layers prepared by oxidizing an organo-silane in an Ar/O_2 *rf* plasma discharge produce parallel alignment for nematic liquid crystals with essentially zero tilt. In addition, if the *rf* plasma system is arranged to produce an Ar/O_2 beam, uniform parallel alignment can now be obtained with the director in the substrate plane at an angle perpendicular to the plane of incidence of the *rf* plasma beam. We have studied the aligning properties of such films using the evanescent wave generated by attenuated total reflection (ATR) on a thin gold film when a surface electromagnetic wave is excited. Liquid crystal cells were constructed on a high index glass prism with a 500 Å gold film and a 200 Å aligning layer. By following the ATR minimum as a function of applied electric field, the tilt at the interface of the liquid crystal and the aligning layer was calculated.

INTRODUCTION

In a previous paper[1] it was shown that surface plasmon resonance techniques can be used to study the interface of a liquid crystal and the aligning layer. ATR spectra were obtained for homeotropic aligned cells using a polyfluorocarbon aligning layer as well as for homogeneous aligned cells using an SiO_2 aligning film. The two indices n_ϵ and n_0 were calculated for one compound, *n*-pentylcyanobiphenyl and good agreement was found for both orientations with published data. In this paper we present our results on the tilt angle at the interface of the undisturbed cell and the change in the tilt when the cell is biased by a square wave voltage. The probe is the evanescent wave emanating from a thin gold film evaporated onto one side of a glass prism. These evanescent waves decay in a fraction of their wavelength, about 3000 Å. Thus the surface layer studied by this method is in this range of thickness.

E. Kretschmann[2] has analyzed the excitation of surface plasmon waves for a glass/metal/vacuum system. If the incident beam is *p*-polarized (TM) the

† Presented at the Eighth International Liquid Crystal Conference, Kyoto, July 1980.

reflected intensity is sharply reduced when the parallel component of the wave vector of light, determined by the angle of incidence, matches the conditions to excite the surface plasmon wave. For details the reader is referred to summary papers by H. Raether[3] and A. Otto.[4] Kretschmann's method for a single film is readily extended to the case where the metal is covered with a thin oxide or polymer film and this has been used to study the optical properties of thin organic layers, down to monolayers.[5-7] In this paper the calculation is extended further to include the case of layers of birefringent material. Tractable solutions can be obtained if the optic axis is in the plane of polarization.

The preparation of uniformly parallel aligned liquid crystal cells using very thin SiO_2 aligning layers deposited by the *rf* plasma beam technique has been described elsewhere.[8,9] The aligning layer is only about 1/40 of the vacuum wavelength but this produces an ATR shift of about 2° and thus the aligning layer must be included in the calculation. To a crude approximation one could regard the evanescent wave as being generated by the glass/Au/SiO_2 system, while information is obtained pertaining to the SiO_2/liquid crystal interface. This is a departure from previous papers in which the metal/organic layer interface is studied directly.

THE ATR METHOD

Figure 1 shows the complete cell in cross section and the light path. The plane of polarization (*p*-polarized) is the plane of the paper and the director is also

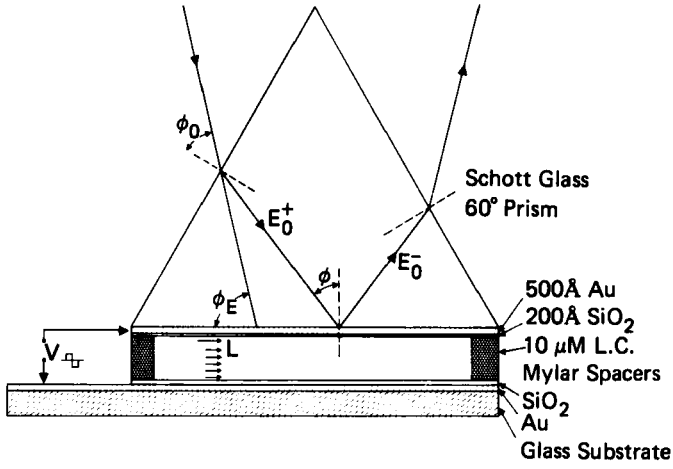

FIGURE 1 An ATR experiment with an operational liquid crystal cell. Cross section through plane of polarization. The "external angle" ϕ_E is used for reference in the following figures. ϕ is the angle of incidence. The geometric relation between ϕ and ϕ_E is accounted for in the computer program: $\phi = \pi/3 - \sin^{-1}(1/n \sin(\phi_E - \pi/6))$.

in this plane. Regarded as an optical system, the cell consists of a glass 60° prism cut from a high index glass (Schott LASF5, $n_A = 1.87625$), a thin evaporated gold film nominally 500 Å, a thin SiO_2 aligning layer deposited by oxidizing a silane in an Ar/O_2 plasma, nominally 200 Å thick and the liquid crystal material. For the unbiased cell, the liquid crystal layer is homogeneous and infinitely thick. The optic axis is in the plane of polarization and parallel to the surface. When a bias voltage is applied the optic axis tilts but remains in the plane of polarization. For numerical calculation it is convenient to consider the liquid crystal as a succession of thin homogeneous layers, their optical constants being determined by the local tilt angle. In our computer program the layer thickness was taken arbitrarily to be 100 Å and it was shown that using thinner layers or more steps does not change the results significantly. Thus the cell is regarded as a stratified multilayer structure. The reflectivity of such structures is discussed in textbooks[10,11] and review papers.[12,13] The case of one birefringent layer was considered for an anisotropic organic crystal[14] but the case of many birefringent layers has not to our knowledge been treated. Our calculations were extended to include both isotropic and anisotropic layers. The method is outlined below in general terms and the derivation is given in an accompanying paper as the algebra is rather extensive.[15]

From the standard boundary conditions, viz. the tangential components of E and H must be continuous across each interface, two linear equations result for the parallel components of E, respectively, H on both sides of the interface. For each medium a relation between H and E follows from the Maxwell equations. Eliminating H, one equation results relating the parallel components of E for the incident and reflected waves on one side of the boundary to those on the other side. The equation is linear and conveniently written as a 2×2 matrix. Combining the two boundaries of one layer then yields a matrix describing the layer. Repeating the process for all layers results in a product of matrices. The final equation relating the parallel components on one side of the multilayer structure to those on the other side can be written as:

$$\begin{pmatrix} E^{+}_{0,x} \\ E^{-}_{0,x} \end{pmatrix} = \prod_{n=0}^{n=N} [M_n] \times \begin{pmatrix} E^{+}_{N+1,x} \exp -ik^{+}_{N+1,z} z_{N+1} \\ E^{-}_{N+1,x} \exp ik^{-}_{N+1,z} z_{N+1} \end{pmatrix}$$

where M_n, the characteristic matrix, is given by

$$M_n = \begin{bmatrix} \dfrac{u_n + u_{n+1}}{2u_n} \exp ik^{+}_{n,z} d_n & \dfrac{u_n - u_{n+1}}{2u_n} \exp ik^{+}_{n,z} d_n \\ \dfrac{u_n - u_{n+1}}{2u_n} \exp -ik^{-}_{n,z} d_n & \dfrac{u_n + u_{N+1}}{2u_n} \exp -ik^{-}_{n,z} d_n \end{bmatrix}$$

Here, d_n is the thickness of the n^{th} film, $d_{n+1} = z_{n+1} - z_n$ and $d_0 = 0$. Superscript + indicates the direction of the incident wave. Superscript − indicates the direction of the reflected wave. $k_{n,z}$ is the normal component of the wave vector in the n^{th} layer. For isotropic layers:

$$k^{+}_{n,z} = k^{-}_{n,z} = \pm\sqrt{\epsilon_n\left(\frac{\omega}{c}\right)^2 - k^2_{0,x}}.$$

For anisotropic layers:

$$k^{+}_{n,z} = -k_{0,x}\frac{\epsilon_{x,z}}{\epsilon_{z,z}} \pm \frac{\sqrt{\epsilon_1\epsilon_2}}{\epsilon_{z,z}}\sqrt{\epsilon_{z,z}\left(\frac{\omega}{c}\right)^2 - k^2_{0,x}}$$

$$k^{-}_{n,z} = k_{0,x}\frac{\epsilon_{x,z}}{\epsilon_{z,z}} \pm \frac{\sqrt{\epsilon_1\epsilon_2}}{\epsilon_{z,z}}\sqrt{\epsilon_{z,z}\left(\frac{\omega}{c}\right)^2 - k^2_{0,x}}$$

$$k_{0,x} = \frac{\omega}{c} n_0 \sin\phi.$$

The sign depends on the convention adopted for the wavefunctions, it must be such that the amplitude of the evanescent wave decays with z. For wavefunctions of the form $\exp i(\omega\tau - \mathbf{k}\cdot\mathbf{r})$ the − sign is the appropriate choice for the incident wave.

The functions u are the generalized relations between H_y and E_x in each layer. For isotropic layers:

$$u_n = \frac{\epsilon_n}{k_{n,z}}.$$

For anisotropic layers:

$$u_n = \pm\sqrt{\frac{\epsilon_1\epsilon_2}{\epsilon_{z,z}\left(\frac{\omega}{c}\right)^2 - k^2_{0,x}}}$$

with the same sign convention as used for the k_z's. The abbreviations $\epsilon_{x,z}$ and $\epsilon_{z,z}$ contain the tilt angle of that layer:

$$\epsilon_{x,z} = (\epsilon_1 - \epsilon_2)\sin\alpha_n\cos\alpha_n$$

$$\epsilon_{z,z} = \epsilon_1\sin^2\alpha_n + \epsilon_2\cos^2\alpha_n$$

ϵ_1 is the component of the permittivity tensor parallel with the optic axis. ϵ_2 is the perpendicular component.

In these experiments there is no wave incident on the last surface and the second term of the E_{N+1} vector is zero. It is then any easy matter to write a

general expression for the reflectivity. Let a matrix M_{ij} represent the result of all matrix products, then

$$R \equiv \frac{E_0^-}{E_0^+} = \frac{E_{0,x}^-}{E_{0,x}^+} = \frac{M_{21}}{M_{11}}.$$

Notice that common terms in each of the layer matrices drop out which reduces computer time significantly. In particular the terms $k_{0,x}(\epsilon_{x,z}/\epsilon_{z,z})$ in the expressions for k_z are common and can be disregarded in the calculation of the exponential terms. Finally, as will be clear, for comparison with experimental data the calculated R must be corrected for the reflectivity and transmission of the glass prism. These corrections were included in the computer program.

RESULTS

Each layer is determined by its values for ϵ and d. For the complete system this forms a large set of parameters. However ϵ and d can be determined for each layer in succession. Figure 2 is a summary of the reflectivity data. The ATR curves were measured in succession for (1) the glass/gold/air system, (2) the glass/gold/SiO_2/air system and (3) the glass/gold/SiO_2/liquid crystal system. To avoid overlap only some of the data for the cell under bias voltage are shown. However, Figures 3–9 show the calculated and experimental data for the complete cell for each applied bias voltage.

The ATR curve for the gold film represents only two matrices. The expres-

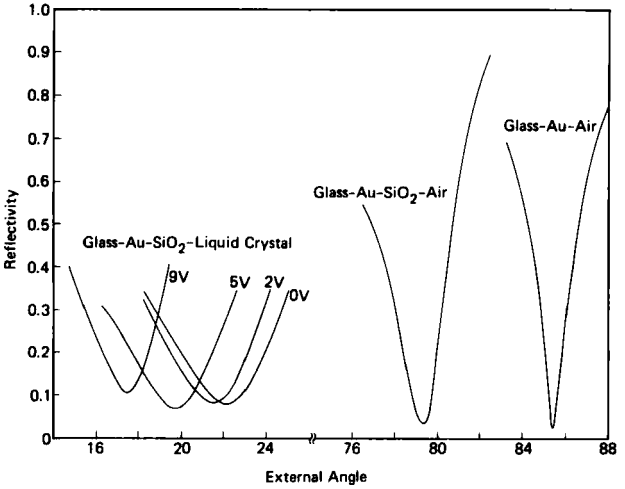

FIGURE 2 The significant part of the ATR curves for Au, Au/SiO_2, and Au/SiO_2/liquid crystal. Plotted is the observed reflectivity vs. the external angle. To avoid overlap only the curves for 0, 2, 5 and 9 volts are shown. For the complete set see Figures 3–9.

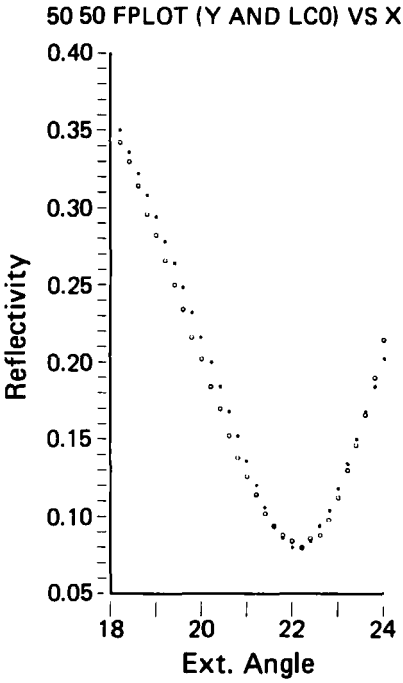

FIGURE 3 Experimental data (O) and calculated ATR curve (●) for the system/glass/Au/SiO_2/LC. The liquid crystal is homogeneous aligned with the director in the plane of polarization. The data was calculated for the experimental values of ϕ_E using $n_\epsilon = 1.745$ and $n_0 = 1.517$.

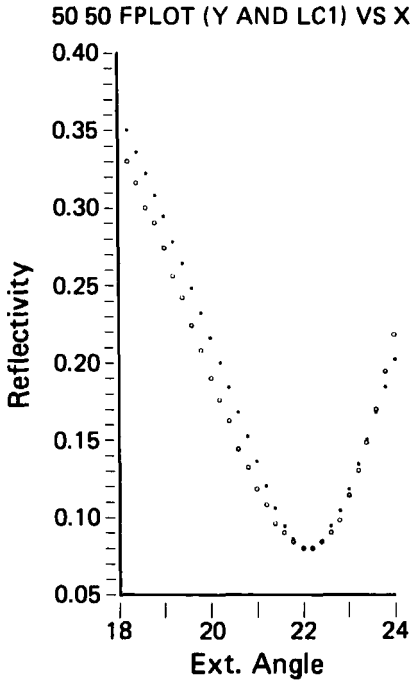

FIGURE 4 Experimental data (O) and calculated ATR curve (●) for the system/glass/Au/SiO_2/LC with 1 volt applied to the cell. The cell is now considered as a stratified medium. The tilt angle changes linearly with the distance to the surface. For the values of the slope see Figure 10.

sion for the reflectivity can be minimized analytically as Kretschmann has shown. For multiple layers this is no longer feasible although Wolter has derived expressions for up to three films. It was decided to use the same numerical approach for all calculations and an APL program was written to evaluate the matrix product for any number of matrices. For the Au film there are still three numerical values to be determined as ϵ is complex. It turned out that ϵ_R is largely determined by the value of ϕ_E minimum, d is largely determined by $R_{\min}$ and the width of the curve largely determines ϵ_I. Thus starting values were found rapidly. After the Au curve was determined, the SiO_2 layer was deposited and the new ATR curve was measured. ϵ_2 and d_2 were calculated from the product of three matrices using ϵ_1 and d_1 previously calculated. It is often possible at this stage to make small changes in ϵ_1 or d_1 to obtain a better fit for both curves. For the cell used in this example the numerical values found were:

$$\epsilon_R = -11.7 \qquad \epsilon_I = -0.80 \qquad d_1 = 420\text{Å}$$

$$n_2 = 1.457 \qquad d_2 = 210\text{Å}$$

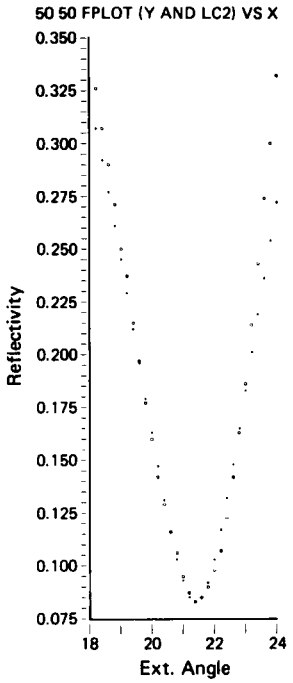

FIGURE 5 As Figure 4 but 2 volt bias applied to the cell.

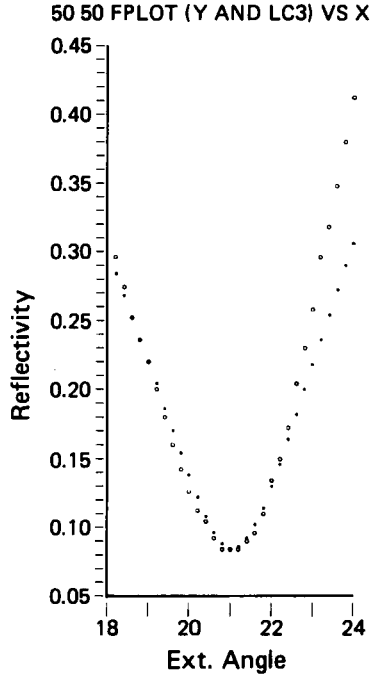

FIGURE 6 As Figure 4 but 3 volt bias applied to the cell.

The cell was then completed and filled. Mylar spacers were used to obtain a cell thickness of about 10 μm and the cell was filled with *n*-pentylcyanobiphenyl (K15 from B.D.H. as received). From the ATR curve for the cell as filled (Figure 3) the two indices were calculated using the product of 4 matrices since for this case d_3 is infinite. The numerical values at 6328Å are:

$$n_\epsilon = 1.745 \qquad n_0 = 1.517 \qquad \Delta n = 0.22$$

The value for n_ϵ agrees closely with that found by us for teflon aligned cells:[1] $n_\epsilon = 1.742$. Data for the refractive indices of this compound have been published and the interpolated values from the B.D.H. catalog are:

$$n_\epsilon = 1.719 \qquad n_0 = 1.528 \qquad \Delta n = 0.19$$

Δn from our data is slightly larger. Presumably alignment by rubbing as used to obtain this published data causes a slight tilt.

At this stage all optical parameters are now known. The tilt angle as a function of distance to the surface can be calculated from the continuum theory and therefore the ATR curve can be calculated for any chosen bias voltage. These calculations were made and it was found that the calculated shift in the

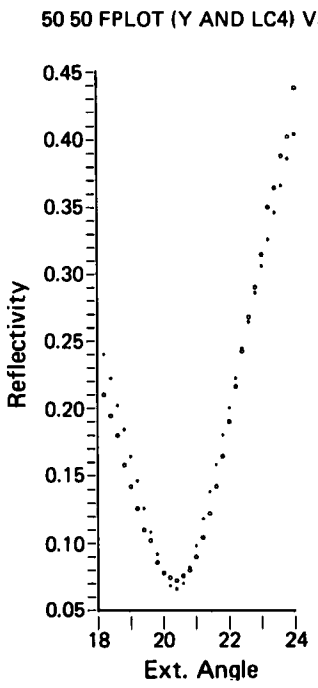

FIGURE 7 As Figure 4 but 4 volt bias applied to the cell.

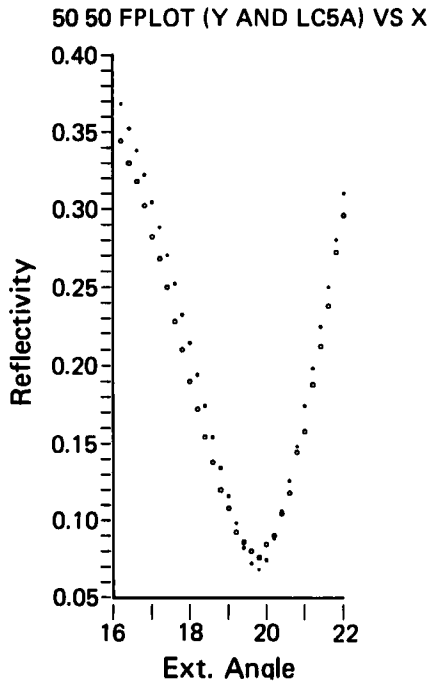

FIGURE 8 As Figure 4 but 5 volt bias applied to the cell.

ATR minimum is much smaller than the shift observed experimentally. Therefore, the process was reversed and the tilt at the surface was determined as a function of the applied bias from the observed ATR curves. It was assumed that the angle at the interface remains zero which is identical to the boundary condition commonly used in obtaining the solution of the Frank Oseen equation. It was further assumed that the tilt changes linearly with distance near the surface for the first 3000Å. Typical Frank Oseen curves are approximately linear over a much larger distance. The computer program now determines a slope, i.e., the derivative of tilt angle with distance such that the calculated ATR curve coincides with the observed curve. All calculations were based on 30 steps of 100Å each. At each 100Å layer the angle defines the tensorial components and therefore there are no other adjustable parameters. These curves are plotted in Figures 3–9 for the bias voltages indicated. It is seen that agreement was obtained. The calculated slopes are plotted versus the bias in Figure 10. For comparison the slope calculated from continuum theory is also shown. The general features of the curves are similar. There is a threshold, below which the tilt remains zero. At the threshold there is a steep change in the tilt followed by a more gradual increase. It is seen that the slope beyond

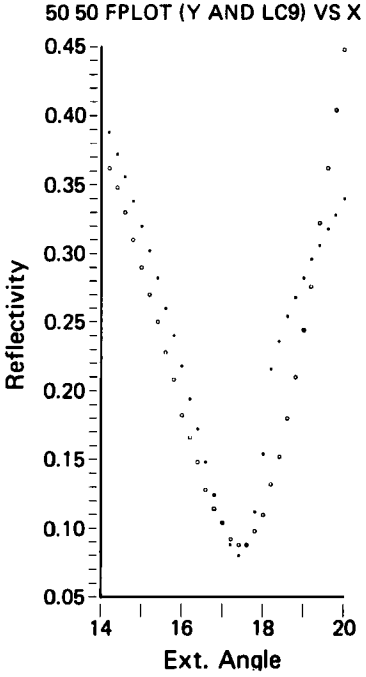

FIGURE 9 As Figure 4 but 9 volt bias applied to the cell.

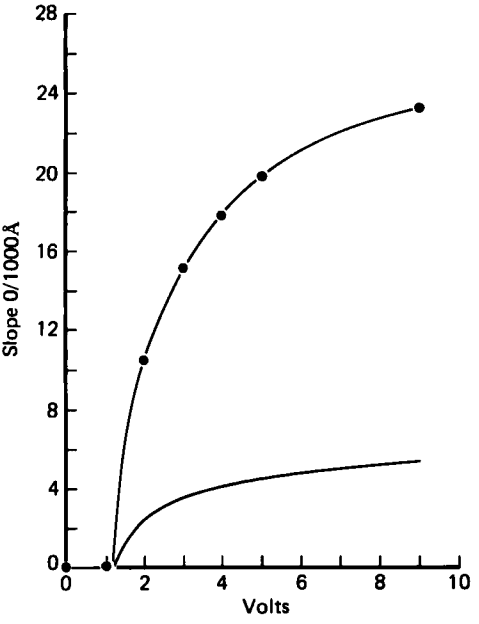

FIGURE 10 The slope of the tilt angle at the surface as determined by Figures 3–9. There exist a threshold value between 1 and 2 volt. Also plotted is the tilt angle calculated from Frank Oseen Theory for equal k's.

threshold increases much faster than that predicted by the continuum theory. The bias voltage was chosen arbitrarily, at present, we have no data to establish the threshold better. From the cell transmission for this material, it is about 1.4V.

DISCUSSION

The discrepancy between the tilt at the surface calculated from observed optical data and that calculated from theory merits further clarification. A qualitative comparison has already been made between the ATR minimum for a homeotropic cell (teflon alignment) and that of a homogeneous aligned cell under large voltage. The homogeneous cell appears to change near the surface much more than expected from theory.[1] The general model used in continuum theory, viz. tilt angle constant at the surface and determined by elasticity within the cell does not differ essentially from the one adopted here. Any other model would depart more from the accepted concepts. Further, the matrix method used to calculate the ATR minimum is also well established. Jacobson[13] has discussed the method in detail including its convergence if the layer thick-

ness is very small compared to the wavelength and the effect of small transition regions at each boundary. Pockrand *et al.*[6] found that for more than six monolayers the effect of the transition region has largely disappeared. Each layer considered in our calculation contains about 20 monolayers. The overall agreement for the refractive indices for cells with either teflon or SiO_2 aligning layers also seems to justify neglecting such transition layers. But there is the possibility of electrolytic reactions at the electrodes which could cause changes in the refractive indices near the surface by establishing a "thick" intermediate layer. Indeed the ATR minimum for the unbiased cell changes by about 0.6° if the cell is subjected to 15 volts for sometime. But this is 10× threshold and near electric breakdown. One cell mistreated in this way, however, still showed about the same shift in the ATR minimum as bias was applied. In normal operation there is no observed shift in the ATR curve at 0 volt bias in cycling to a voltage below breakdown and returning. Hence we feel these effects have a negligible influence on our results.

In conclusion, we feel that the ATR method is a good technique for studying the aligning properties of molecules at a metal interface, and in particular the aligning properties of liquid crystals. Our results also show convincingly, that the molecules rotate faster than calculated by Frank Oseen Theory. Hopefully this will stimulate further theoretical work to understand this discrepancy.

References

1. J. D. Swalen and G. J. Sprokel, *Physics and Chemistry of Liquid Crystals,* Plenum (1980).
2. E. Kretschmann, *Z. Physik.*, **241,** 313 (1971).
3. H. Raether, *Physics of Thin Films*, **9,** 145 (1977).
4. A. Otto, *Spectroscopy of Surface Polaritons, Optical Properties of Solids*, Elsevier (1976).
5. J. G. Gordon and J. D. Swalen, *Optics Comm.*, **22,** 374 (1977).
6. I. Pockrand, J. D. Swalen, J. G. Gordon and M. R. Philpott, *Surface Science*, **74,** 237 (1977).
7. I. Pockrand, J. D. Swalen, R. Santo, A. Brillante and M. R. Philpott, *J. Chem. Phys.*, **69,** 4001 (1978).
8. G. J. Sprokel, *Physics and Chemistry of Liquid Crystals,* Plenum (1980).
9. G. J. Sprokel, *J. Electronic Mat.*, **9,** (3) 651 (1980).
10. M. Born and E. Wolf, *Principles of Optics*, Pergamon (1975).
11. O. S. Heavens, *Optical Properties of Thin Solid Films*, Dover (1965).
12. H. Wolter, *Optik dünner Schichten, Handbuch der Physik*, **XXIV,** 461.
13. R. Jacobson, *Light reflection from films of Continuously varying refractive index*, Progress in Optics V, 249 (1966).
14. M. R. Philpott and J. D. Swalen, *J. Chem. Phys.*, **69,** 2912 (1978).
15. G. J. Sprokel, *Mol. Cryst. Liq. Cryst.*, 39 (1981).